CR-137778

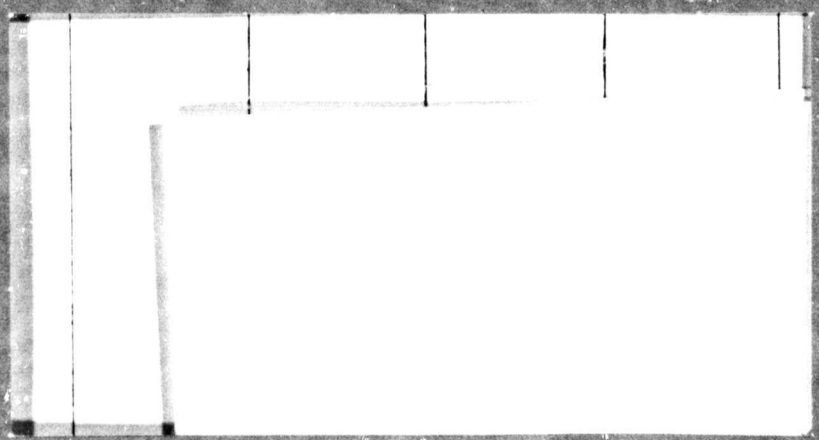




dynatherm
CORPORATION

CR-137778

DTM-75-6

# FINAL REPORT

for

# JET PUMP ASSISTED ARTERY

October 31, 1975

Prepared under Purchase Order A12056B(MW)

for

NASA Ames Research Center
Moffett Field, California

by

Dynatherm Corporation
One Industry Lane
Cockeysville, Maryland

## TABLE OF CONTENTS

# I. INTRODUCTION AND SUMMARY

This report describes the work performed by Dynatherm Corporation under NASA-ARC Purchase Order Number A12056(MW). The program was initiated on April 1, 1975 and completed on September 5, 1975.

The performance potential of an arterial heat pipe and the problems associated with its priming are well known. In state-of-the-art arterial heat pipes, priming is accomplished either through surface tension forces or through temperature induced differences in saturation pressure (Clapeyron priming).

During this program, a different mechanism was investigated for priming an artery and for maintaining it primed. This concept utilizes a capillary driven jet pump to create the necessary suction to fill the artery. Basically, the jet pump consists of a venturi or nozzle-diffuser type constriction in the vapor passage. The throat of this venturi is connected to the artery. Thus vapor, gas, liquid, or a combination of the above is pumped continuously out of the artery. As a result, the artery is always filled with liquid and an adequate supply of working fluid is provided to the evaporator of the heat pipe.

The objective of this program was to provide a proof-of-principle of this concept. Toward this objective, a venturi was designed whose dimensions were compatible with the mass flow rates encountered in a typical arterial heat pipe. Initially, air was used to verify its performance in terms of suction pressure and pressure recovery. The venturi was then incorporated as a jet pump in the proof-of-principle experiment which utilized water vapor in a simulated heat pipe environment. The results of this experiment have shown both through visual observation and through increased pipe performance that the jet pump has the ability to maintain a primed artery even against a substantial adverse gravity gradient.

## II. JET PUMP MODEL

In order to describe arterial priming by means of a jet pump, it is useful to review the pressure and temperature distribution in a regular arterial heat pipe as shown in Figure II-1. The representation is highly schematic. A centrally located artery is shown but bridges and secondary wicks have been omitted. Also, the flow resistance in the vapor path is indicated schematically by a "lumped" flow resistance. The artery is shown to be completely filled. The following relations between pressures then apply:

$$P_v(T_e) = P_v(T_c) + \Delta P_v \qquad \text{II-1}$$

where $\Delta P_v$ is the viscous and/or dynamic pressure loss in the vapor flow and where the symbol $P_v(T)$ indicates saturation pressure at T.

$$P_v(T_e) = P_{l,e} + \Delta P_{cap} \qquad \text{II-2}$$

where $\Delta P_{cap}$ is the capillary pressure head developed by the wick.

$$P_{l,e} = P_{l,c} - \Delta P_l - \Delta P_{grav} \qquad \text{II-3}$$

where $\Delta P_l$ is the viscous and/or dynamic pressure loss in the liquid flow and $\Delta P_{grav}$ represents the gravity head.

$$P_{l,c} = P_v(T_c) \qquad \text{II-4}$$

The last equation assumes, for convenience, that no capillary head exists across the wick at the condenser. Equations II-1 through II-4 may be combined to yield the well known pressure balance in a heat pipe:

$$\Delta P_{cap} = \Delta P_l + \Delta P_v + \Delta P_{grav} \qquad \text{II-5}$$

An arterial heat pipe will function in the described mode only if the artery is

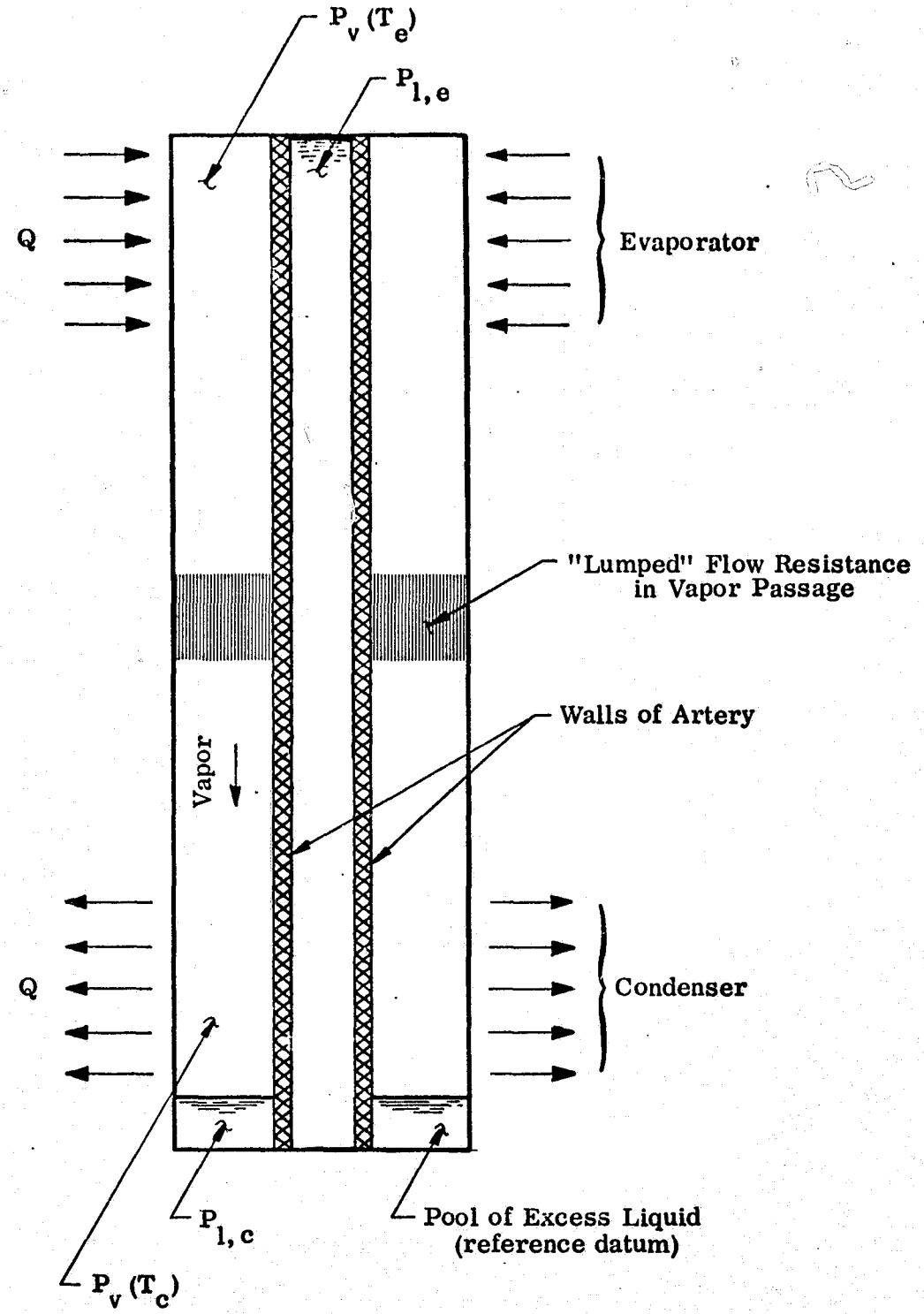


FIGURE II-1

SCHEMATIC OF ARTERIAL HEAT PIPE

completely filled. A partially filled artery (or one which contains a bubble) is not stable since the pressures in the liquid and vapor cannot be easily balanced. This is illustrated in Figure II-2 which is a close-up of the evaporator section of an artery containing a bubble. The bubble will either collapse, be stable, or grow depending on the relative magnitude of the pressures inside and outside the bubble.

$$P_{l,e} > P_b - \frac{2\sigma}{R} \qquad \text{bubble collapses}$$

$$P_{l,e} = P_b - \frac{2\sigma}{R} \qquad \text{bubble is stable} \qquad \text{II-6}$$

$$P_{l,e} < P_b - \frac{2\sigma}{R} \qquad \text{bubble grows}$$

The pressure in the bubble is the sum of the partial pressures of vapor and any non-consensible gas which might be present.

$$P_b = P_{v,a} + P_{gas} \qquad \text{II-7}$$

The pressure of the liquid $P_{l,e}$ is given by Equations II-3 and II-4 which yield:

$$P_{l,e} = P_v(T_c) - \Delta P_l - \Delta P_{grav} \qquad \text{II-8}$$

Combining Equations II-6, II-7, and II-8 gives the following stability criterion for a partially filled artery:

$$P_{v,a} \lesseqgtr P_v(T_c) - \Delta P_l - \Delta P_{grav} - P_{gas} + \frac{2\sigma}{R} \qquad \text{II-9}$$

Examination of Equation II-9 indicates a number of options which are available to prime an artery. If the heat pipe is approximately isothermal, the partial pressure of the vapor in the artery $P_{v,a}$ is equal or slightly smaller than the saturation vapor pressure at the condenser. Thus, the artery will prime if:

$$\Delta P_l + \Delta P_{grav} + P_{gas} < \frac{2\sigma}{R} \qquad \text{II-10}$$

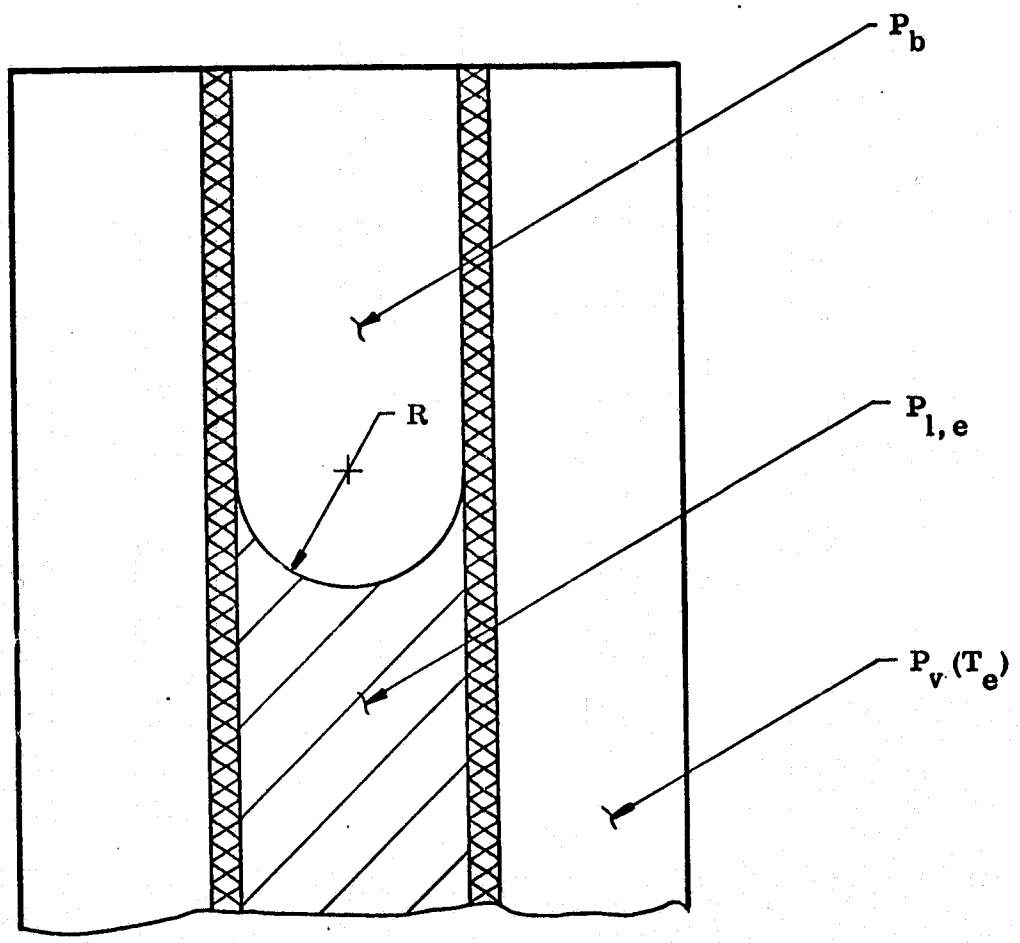


FIGURE II-2

EVAPORATOR SCHEMATIC OF PARTIALLY FILLED ARTERY

This approach implies small loads and gravity heads during priming. In addition, no noncondensible gas should be present. This has been the traditional technique of priming arterial heat pipes (Ref. 1). A variation of this approach is to vent the noncondensing gas during priming. This was accomplished by Enninger through priming foils (Ref. 2).

Another approach involves the lowering of the partial pressure of the vapor $P_{v,a}$ through subcooling the liquid in the artery until the inequality of Equation II-9 is satisfied (Clapeyron Priming, Ref. 3). It works satisfactorily in the absence of noncondensibles. But when gas is present, it remains trapped in the artery and may cause depriming when the load or the environment is changed.

The approach presented here is also based on lowering the partial pressure of the vapor in the unfilled part of the artery. However, it is achieved through the continuous suction of a small capillary jet pump located in the vapor passage of the heat pipe. A typical, yet schematic, configuration of a jet assisted arterial heat pipe is shown in Figure II-3. The heat pipe is similar to the schematic of Figure II-1, except that the lumped flow resistance in the vapor passage has been replaced by a venturi. Also, a suction line is shown from the interior of the artery to the "throat" of the venturi. The suction creates a reduced pressure (and temperature) inside the artery which is required according to Equation II-9 to prime the artery and maintain it primed.

The operation of the jet pump requires, inherently, a pressure drop in the motive stream ($P_v(T_e) - P_v(T_c)$). This pressure drop is equivalent to an additional flow resistance in the vapor flow (in addition to any viscous or dynamic losses). Associated with that pressure drop is a temperature difference between evaporator and condenser. Since the driving force for the jet pump is derived from the capillary pressure rise at the evaporator, the overall pressure drop cannot exceed the capillary head $\Delta P_{cap}$ of the wick. The associated temperature difference is only a fraction of a degree if a high pressure working fluid such as ammonia is employed.

In addition to the schematic representation, Figure II-3 also shows a close-up of a possible jet pump design. It consists of an annular constriction of the vapor path

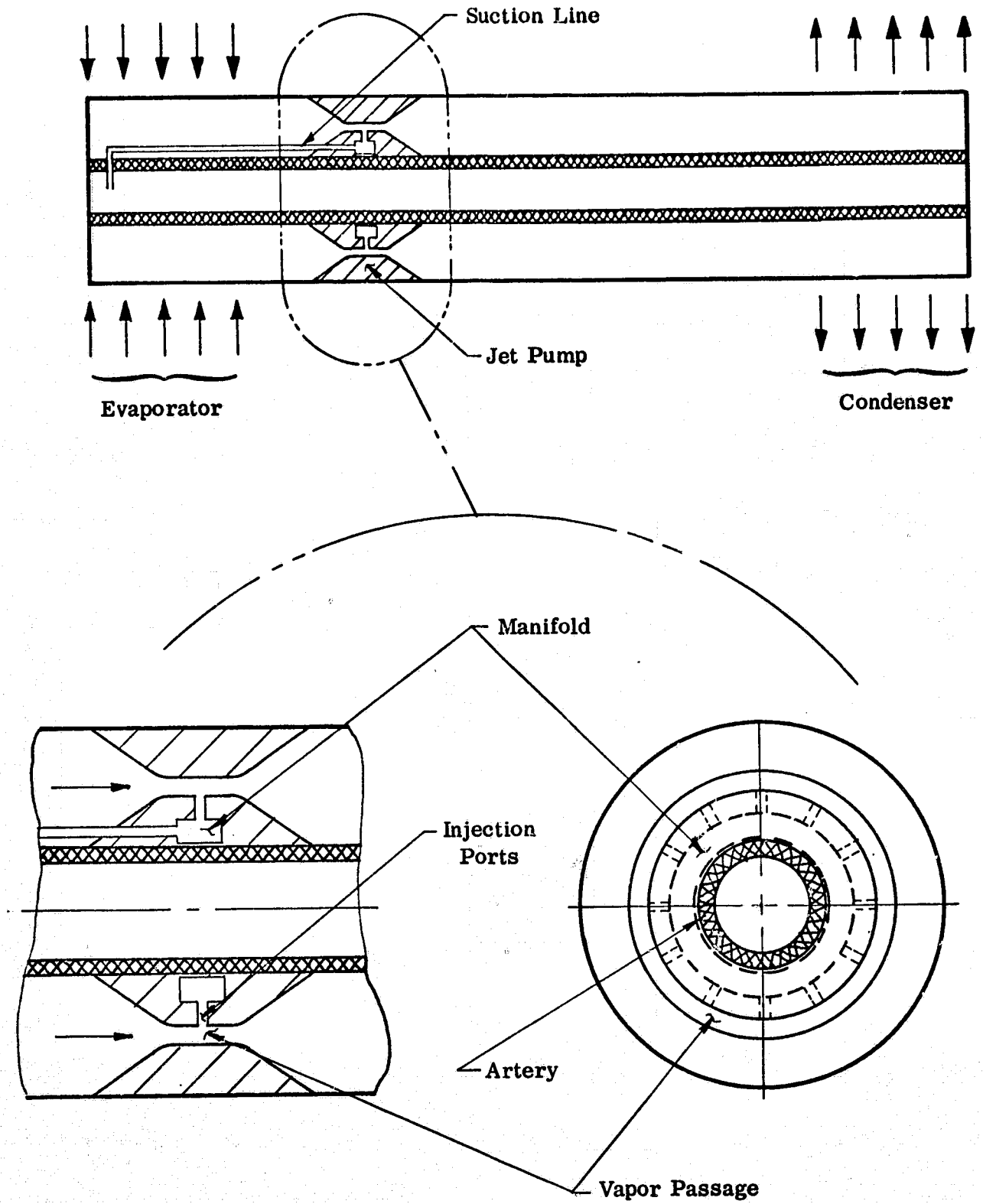


FIGURE II-3

JET ASSISTED ARTERIAL HEAT PIPE

located between evaporator and condenser. One side of the constriction contains a circular manifold from which radial injection ports lead to the vapor stream. A capillary tube connects the artery to the manifold.

A jet assisted arterial heat pipe can assume several other configurations. One possibility is a capillary loop in which the artery and the vapor flow passage are physically separated. In either case, the principal components are:

- An arterial wick capable of supporting viscous and gravitational pressure drops in the liquid and the suction induced pressure drop in the vapor.
- A venturi in the vapor passage.
- A small tube leading from the interior of the artery to the "throat" of the venturi.

The operation of a capillary jet pump is illustrated diagrammatically in Figure II-4. Vapor from the evaporator representing the "motive" fluid enters a converging nozzle at point 0. The vapor is initially at the saturation pressure $P_v(T_e)$ of the evaporator. As it enters the converging nozzle 0-1, it is accelerated and its pressure drops to $P_1$. The vapor or liquid to be pumped enters through the suction port at point 1. This fluid is then entrained by the higher velocity vapor stream. The velocity in the mixing section increases, and this is accompanied by a further pressure decrease. The mixture enters a diffuser at point 2. The function of the diffuser is to slow the fluid down and to increase the static pressure. The pressures at points 0 and 3 are the saturation pressures at evaporator and condenser temperatures, respectively. Note that the pressure ($P_1$) at the suction point 1 is less than either one of the two saturation pressures. Thus, if the suction line is connected with the inside of the artery, a reduced pressure in accordance with the stability criterion (Equation II-9) can be maintained.

For ease of analysis, the venturi was divided into three main sections -- the nozzle, mixing section, and the diffuser (see Figure II-4). Nozzle and diffuser efficiencies were defined and incorporated in the analytical models as:

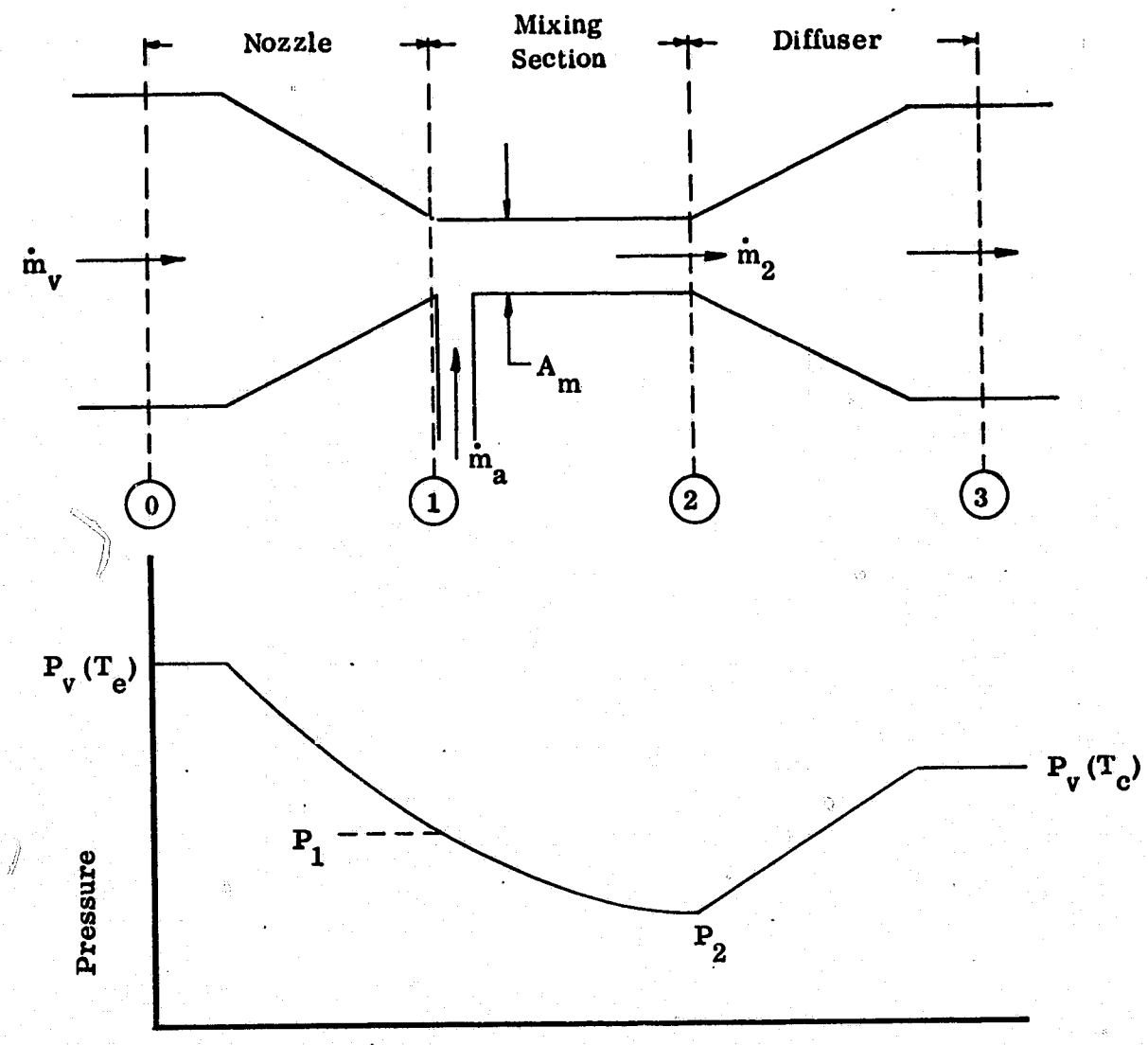


FIGURE II-4

DIAGRAMMATIC SKETCH OF JET COMPRESSOR

$$\eta_n = \frac{(\Delta KE)_{actual}}{(\Delta KE)_{ideal}} \qquad \text{II-11}$$

$$\eta_d = \frac{(\Delta P)_{actual}}{(\Delta P)_{ideal}} \qquad \text{II-12}$$

where $\Delta KE$ is the change in kinetic energy in the converging nozzle and $\Delta P$ is the pressure recovery in the diffuser.

The conditions at the entrance to the nozzle are defined by the operating condition of the evaporator.

$$P_0 = P_v(T_e) \qquad \text{II-13}$$

In order to maintain a primed artery the pressure at the throat of the venturi must be less than the liquid pressure in the artery.

$$P_1 \leq P_{l,e} \qquad \text{II-14}$$

Since the liquid and vapor pressures in the evaporator differ by $2\sigma/r$, the required expansion in the nozzle must be:

$$P_1 \leq P_v(T_e) - \frac{2\sigma}{r} \qquad \text{II-15}$$

Secondly, the overall pressure loss must not exceed the available capillary pumping:

$$\Delta P_{loss} < \frac{2\sigma}{r} \qquad \text{II-16}$$

State 1-S is defined by the T-S diagram shown in Figure II-5. (Tabulated thermodynamic properties are used to describe the state of the vapor. The model could be simplified by employing the ideal gas law for the state of the vapor. Numerically, this leads to almost identical results for the case of water vapor.) It is the state reached by isentropic expansion from $P_0$ to $P_1$. With $P_{1,s}$ and $S_{1,s}$ known; i.e.:

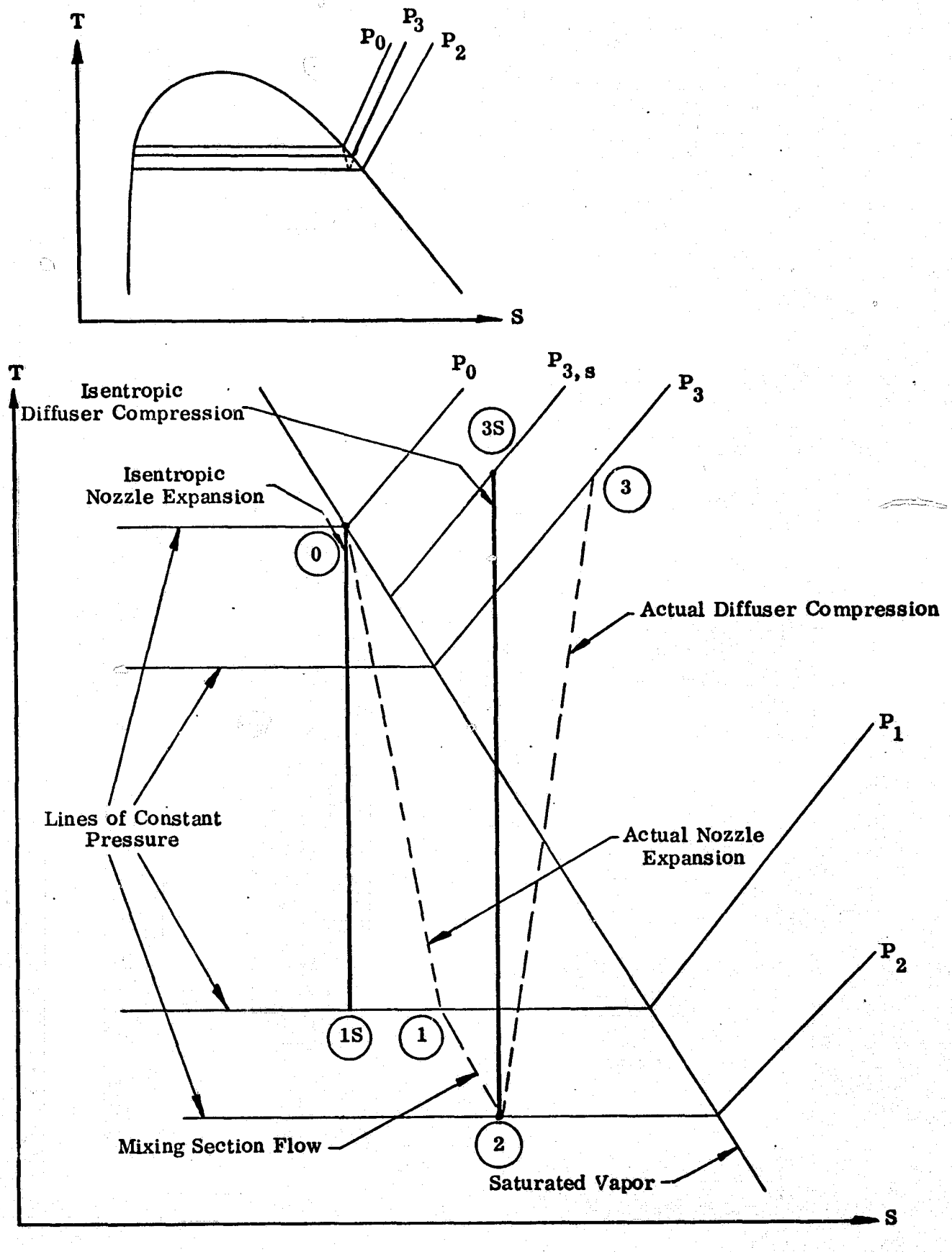


FIGURE II-5

T-S DIAGRAM REPRESENTATION OF VENTURI FLOW

$$P_{1,s} = P_1 \qquad \text{II-17}$$

$$S_{1,s} = S_0 \qquad \text{II-18}$$

State 1-S is determined.

By definition of nozzle efficiency:

$$\eta_n = \frac{(\Delta KE)_{actual}}{(\Delta KE)_{ideal}} = \frac{\left(\frac{V_1^2}{2} - \frac{V_0^2}{2}\right)_{actual}}{\left(\frac{V_{1,s}^2}{2} - \frac{V_0^2}{2}\right)_{ideal}} \qquad \text{II-19}$$

and with the aid of the energy equation,

$$\frac{V_{1,s}^2}{2} - \frac{V_0^2}{2} = h_0 - h_{1,s} \qquad \text{II-20}$$

the velocity $V_1$ can be determined.

A simple expression for the change in entropy between states 1-S and 1 can be derived if state 1 always lies within the saturation region:

$$\Delta S_{1,s} = \frac{(1 - \eta_n)(h_0 - h_{1,s})}{T_1} \qquad \text{II-21}$$

With the pressure and entropy known, state 1 is completely defined. The venturi throat area can be determined using continuity.

$$A_1 = \frac{\dot{m}_1}{\rho_1 V_1} \qquad \text{II-22}$$

where $\dot{m}_1$ is the mass flow rate of the vapor which is given by the heat pipe transport.

When modeling the mixing section, a few simplifying assumptions were made. The density was assumed constant and friction losses were neglected (the assumed

section length was very small). Errors associated with these assumptions were found to be on the order of 1%. For perpendicular mass injection, the momentum yields the following expression for the pressure loss in the mixing section:

$$P_2 - P_1 = (\Delta P)_{\text{mass add}} = \frac{1}{A_1}\left(\dot{m}_1 V_1 - \dot{m}_2 V_2\right) \qquad \text{II-23}$$

where:

$$V_2 = \frac{\dot{m}_1 (1 + y)}{\rho_1 A_1} \qquad \text{II-24}$$

$$\dot{m}_2 = \dot{m}_1 (1 + y) \qquad \text{II-25}$$

and $(\Delta P)_{\text{mass add}}$ is the pressure loss due to mass addition. The term $(\dot{m}_1 V_1 - \dot{m}_2 V_2)$ is the change in momentum of the flow, and y is the ratio of injected flow to main flow. Knowing the pressure and density at point 2 defines that state.

The diffuser is the most important section since it determines the pressure recovery. The efficiency of the diffuser depends heavily on the divergence angle and area ratio. With the aid of the T-S diagram of Figure II-5, the diffuser flow is described.

Given the diffuser efficiency, exit area, and mass flow, the flow properties at state 3 can be determined. Unfortunately, a closed form solution does not exist. Using the definition of diffuser efficiency:

$$\eta_d = \frac{P_3 - P_2}{P_{3,s} - P_2} \qquad \text{II-26}$$

the continuity equation:

$$V_3 = \frac{\dot{m}_2}{\rho_3 A_3} \qquad \text{II-27}$$

and the energy equation:

$$h_3 + \frac{V_3^2}{2} = h_2 + \frac{V_2^2}{2} = \text{constant} \qquad \text{II-28}$$

and iterating, state 3 can be found.

With the help of this analytical model, the required dimensions and performance of a typical venturi were established. A water heat pipe operating at 66°C was used as the reference design for the proof-of-principle experiment. Conditions representative of this experiment and some derived parameters are given in Table II-1.

| Derived Parameter | Entrance Nozzel | Exit Nozzel | Exit Mixing Section | Exit Diffuser |
|---|---|---|---|---|
| Temperature ($^{o}$C) | 66.35 | 64.51 | 64.44 | 66.29 |
| Pressure ($N/m^2 \times 10^4$) | 2.620 | 2.413 | 2.406 | 2.541 |
| Vapor Velocity (m/sec) | 16.00 | 153.1 | 155.1 | 17.46 |
| Mass Flow Rate ($kg/sec \times 10^{-5}$) | 8.536 | 8.536 | 8.621 | 8.621 |
| Vapor Quality (%) | 100.0 | 99.60 | 99.60 | Superheated |
| Area ($m^2 \times 10^{-6}$) | 31.67 | 3.565 | 3.565 | 31.67 |

| Parameter | Design |
|---|---|
| Fluid | Water |
| Temperature ($^{o}$C) | 66.00 |
| Heat Pipe Diameter (cm) | 0.635 |
| Wick Mesh Size | 200 |
| Input Power (watts) | 200 |
| Nozzel Efficiency (%) | 90 |
| Diffuser Efficeincy (%) | 70 |
| Mass (Vapor) Injection ($kg/sec \times 10^{-7}$) | 8.536 |

**TABLE II-1**

**DERIVED AND DESIGN PARAMETERS FOR PROOF-OF-PRINCIPLE EXPERIMENT**

## III. VENTURI DEVELOPMENT

The venturi design parameters were based on arbitrarily chosen conditions to be representative of the proof-of-principle experiment. These are given in Table II-1. Nozzle and diffuser efficiencies were chosen to be:

$$\eta_n = 0.9$$

$$\eta_d = 0.7$$

These values are well within the state-of-the-art for venturi designs. The diffuser divergence angle is the major parameter affecting $\eta_d$. The first venturi was designed with a diffuser divergence angle of 10 degrees and had a straight mixing section.

Testing with air indicated that the useful pressure drop through the nozzle was slightly greater than was predicted. An additional pressure decrease was experienced in the straight section which resulted from the "vena constricta" effect. The total pressure loss (measured in percent of useful pressure drop) was 54% compared to the predicted value of 37% based on assuming $\eta_n = 0.9$ and $\eta_d = 0.7$. The test configuration is shown in Figure III-1.

A second venturi was designed using the information obtained during testing of the first model. Its parameters are given in Table III-1. The diffuser divergence angle was decreased to 5 degrees and the straight section was eliminated. Tests were conducted using air to verify pressure loss assumptions. One throat static tap was employed and located approximately one-half of a throat diameter downstream from the throat. This static tap was later employed as the artery pumping port. Testing indicated that, at the design point (i.e., 6 liters/minute corresponding to 200 watts), the pressure drop in the nozzle was $2.83 \times 10^3$ N/m$^2$ which is more than the capillary pumping of the 200-mesh screen ($2.06 \times 10^3$ N/m$^2$). The total pressure loss was 38% of the nozzle pressure drop. The results are shown in Figure III-2. This performance of the venturi was felt acceptable for the proof-of-principle experiment.

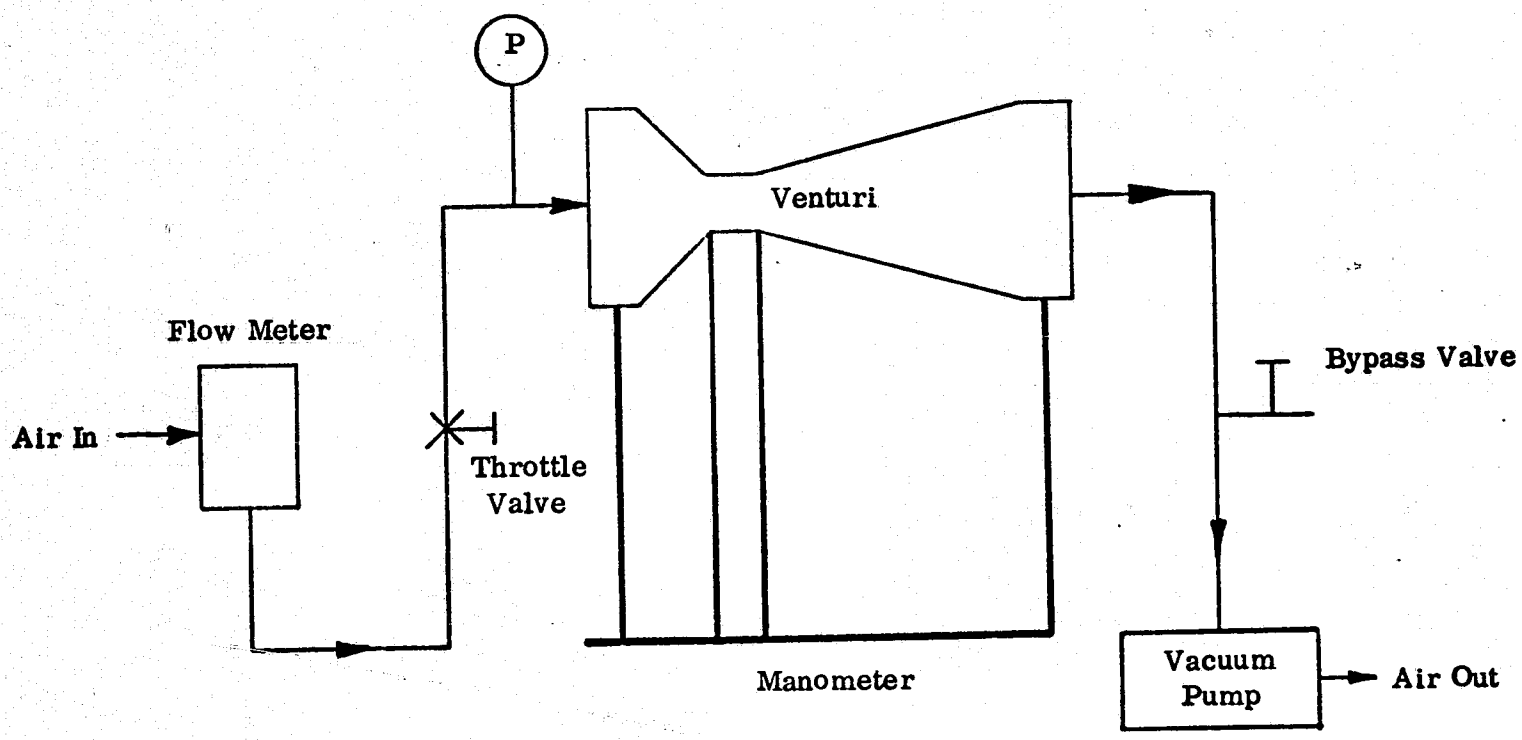


FIGURE III-1

SETUP FOR AIR FLOW TEST

TABLE III-1

| | | |
|---|---|---|
| Nozzle Inlet Diameter | : | 0.635 cm (0.250 inch) |
| Nozzle Convergence Angle | : | 20 degrees |
| Diffuser Divergence Angle | : | 5 degrees |
| Diffuser Exit Diameter | : | 0.635 cm (0.250 inch) |

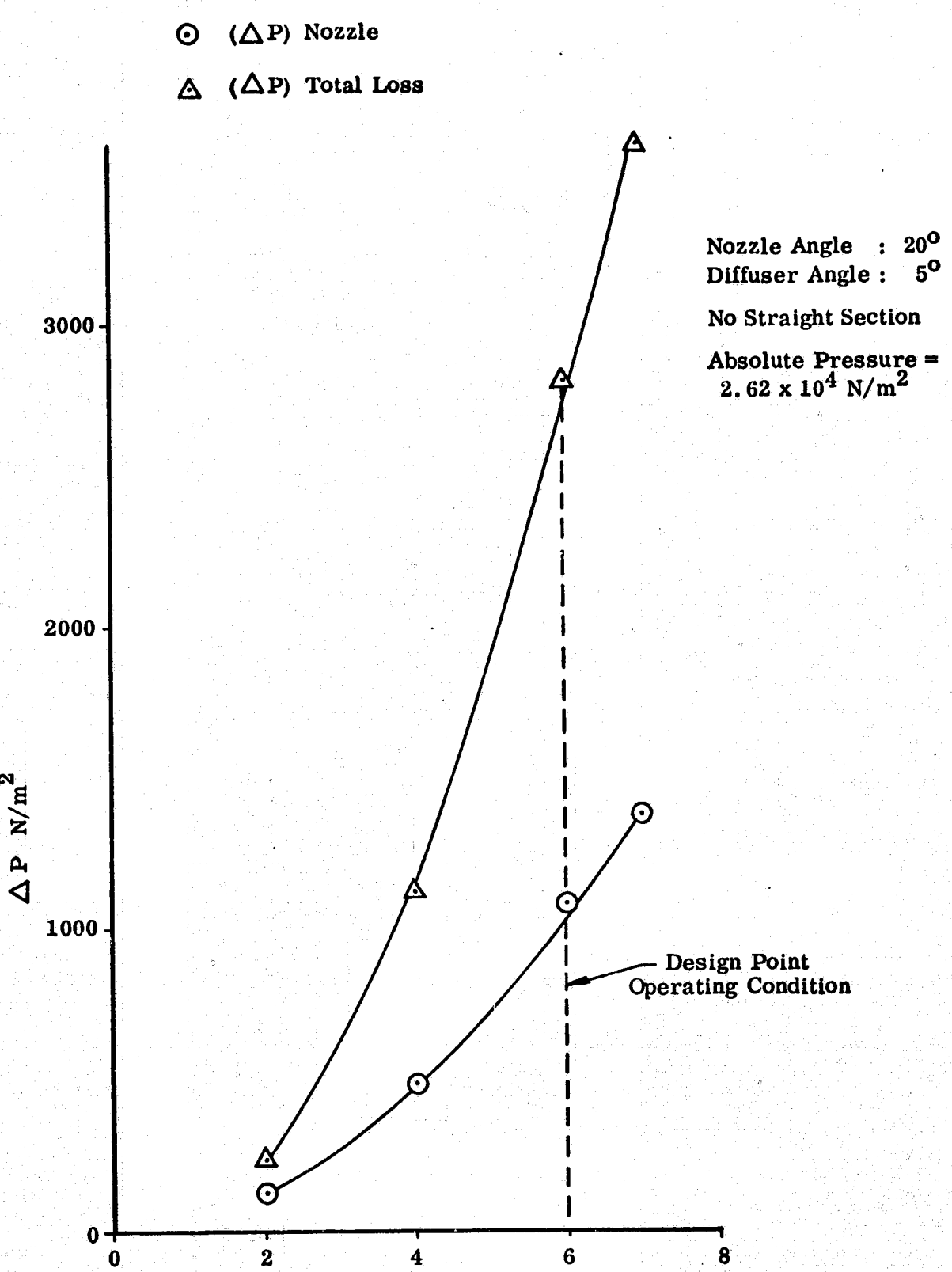


FIGURE III-2

VENTURI PERFORMANCE

# IV. PROOF-OF-PRINCIPLE EXPERIMENT

## IV-1 Objective

The objective of this experiment was to demonstrate the ability of the jet pump to prime an artery and to maintain it primed under load in a simulated heat pipe environment.

## IV-2 Test Setup

The overall test setup is shown in Figure IV-1. It consisted of a closed loop with a liquid pool at the bottom leg. The right leg represented the evaporator which was fed from the pool by capillary forces. The jet pump was located directly above the evaporator. The left leg served as the condenser. Several thermocouples were located at the evaporator and other sections of the loop. The system pressure was monitored with a gage. Two sight glasses were installed -- one permitted observation of the liquid level in the pool; the other one permitted observation of the suction of the jet pump. The working fluid was distilled water. Most tests were conducted at a vapor temperature of 66$^{o}$C. The individual sections are described below in more detail.

### IV-2.1 Evaporator

The evaporator consisted of a 2.54 cm diameter by 15.24 cm long stainless steel tube. A resistance heater was wound around the upper 6.35 cm of the tube. The level of the pool could be varied from the bottom of the heater down to 7.62 cm below the heater.

A wire mesh outer wick lined the inside of the evaporator tube. It consisted of tight wraps of 200-mesh stainless steel screen which was "ebonaled" (*) to improve wetting by water. Throughout the test period, various numbers of wraps were used. Initially, four wraps were used to line the evaporator tube. Testing indicated

---

*Ebonal is a tradename of the Enthone Company for a black oxide which has excellent wetting properties.

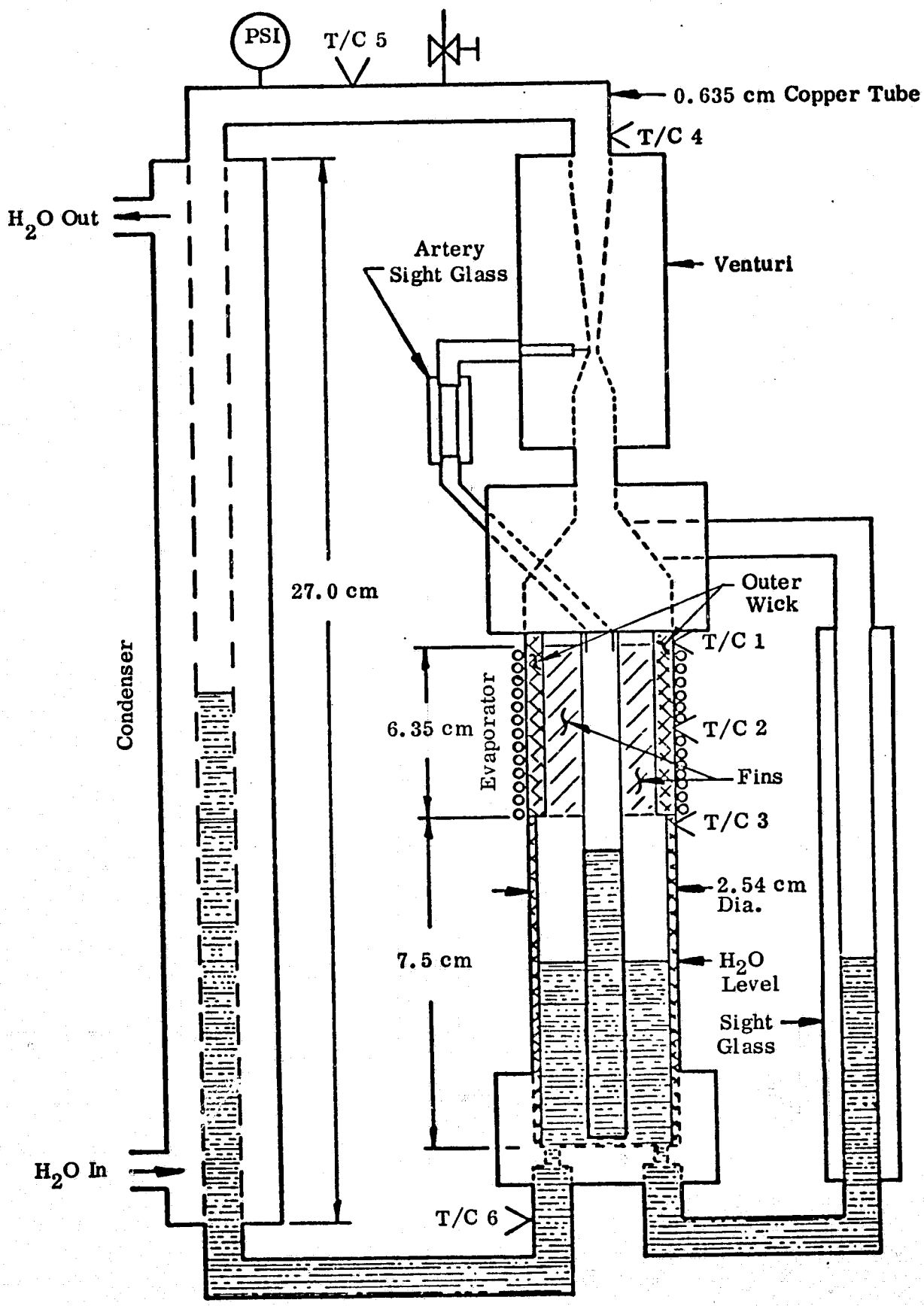


FIGURE IV-1

PROOF-OF-PRINCIPLE TEST SETUP

the transport was much too high even without the artery. The wick configuration was then changed to two wraps in the heater section and one in the adiabatic and pool section below the evaporator. The final wick configuration consisted of four wraps in the heater section and one layer in the adiabatic section.

### IV-2.2 Artery

The artery was also constructed at 200-mesh stainless steel screen. It extended along the length of the evaporator tube. The artery feeds the outer wick in the heater section via three fins which were also constructed of 200-mesh stainless steel screen. Figure IV-2 shows the details of artery design.

### IV-2.3 Venturi

The venturi was the same design as used in the air experiments. It was machined from brass. The venturi, the injection port, and the brass adapter to the evaporator are shown in Figure IV-3.

### IV-2.4 Condenser

The condenser consisted of the 0.645 cm diameter down leg of the loop. Heat was removed through a counterflow water jacket surrounding the condenser tube. The condenser was later changed to a larger diameter (2.56 cm) but shorter (10.2 cm) tube which was located above the original condenser. This allowed an increase in system transport and prohibited subcooling of the returning liquid.

## IV-3 Test Results

### IV-3.1 General

The test results can be grouped into three categories:

- Visual observation of priming
- Increase in performance over unprimed artery
- Recovery from burnout

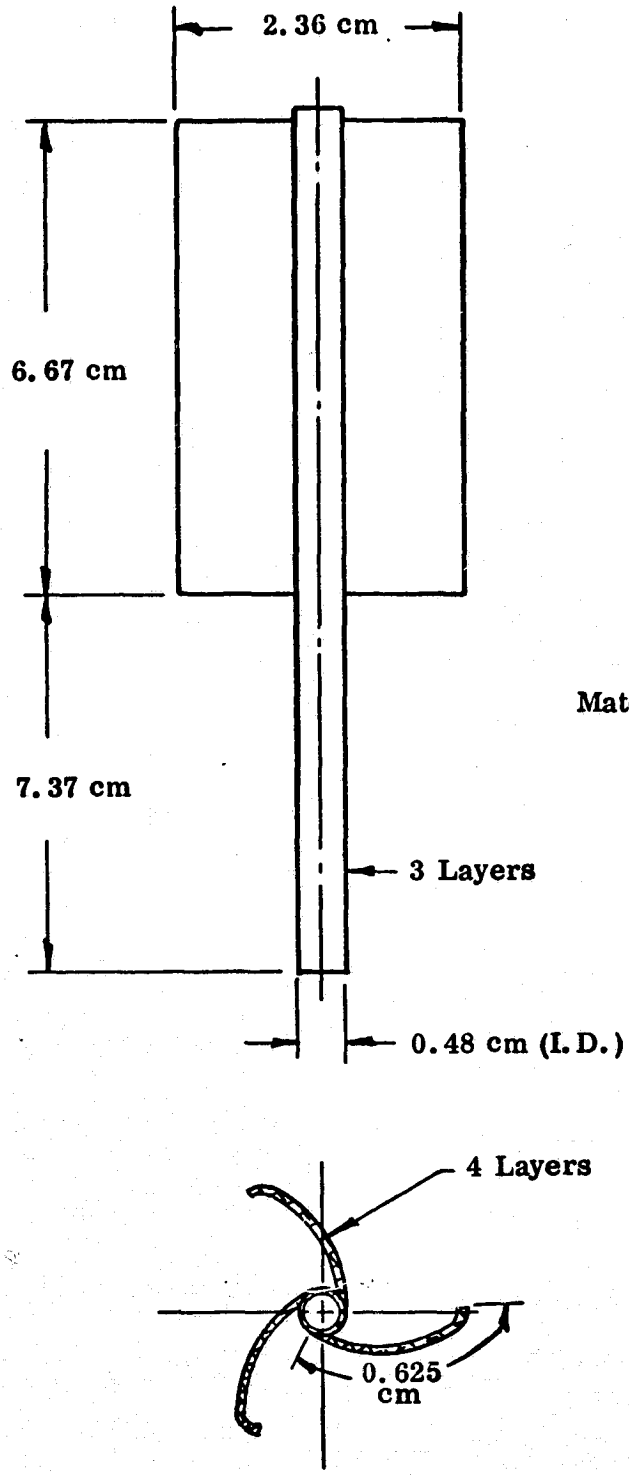


Material: 200-Mesh SS Screen

FIGURE IV-2

ARTERY DESIGN

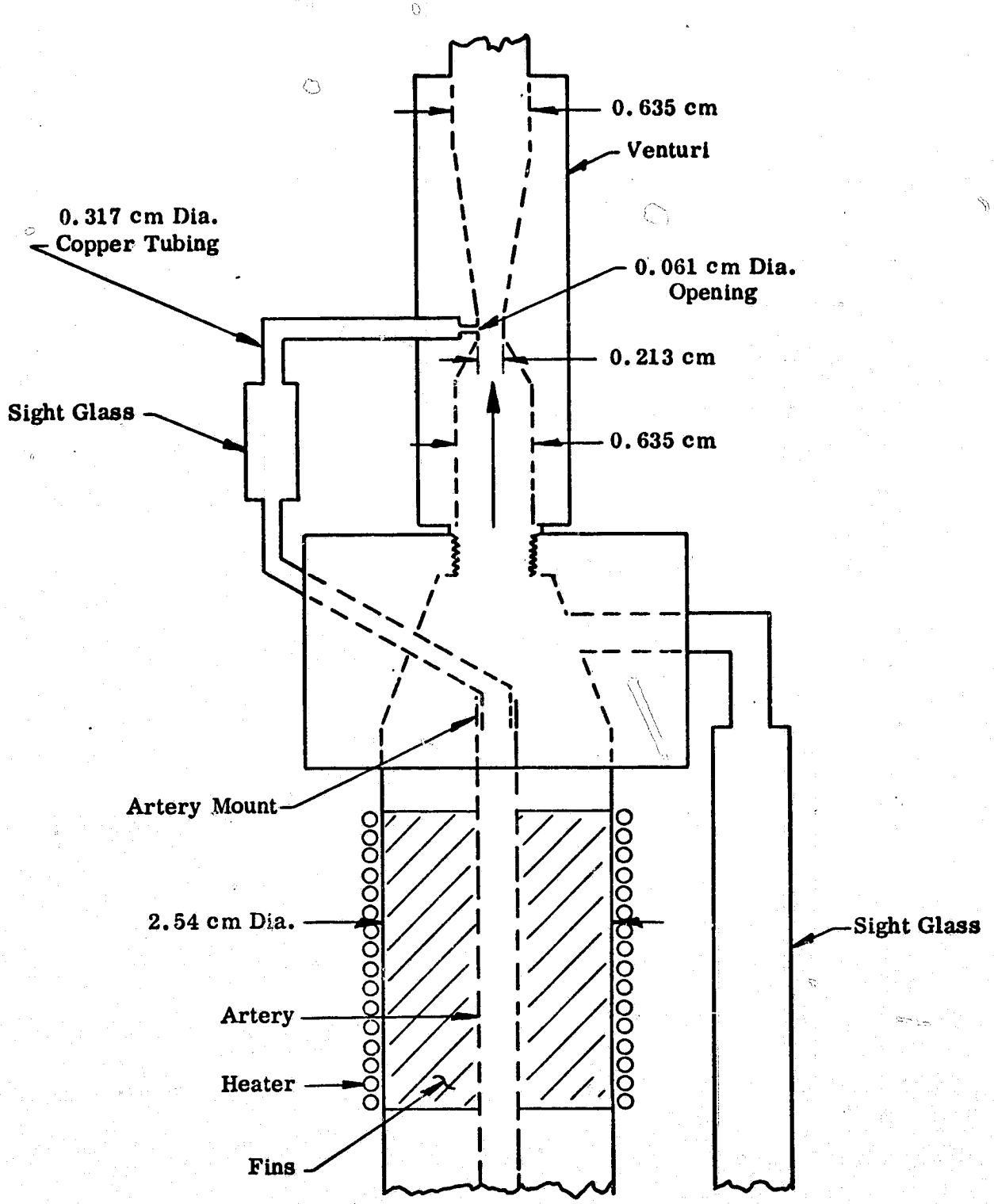


FIGURE IV-3

JET PUMP

This first section presents a discussion of visual observations and general comments regarding the operation of the test loop.

The first step in the test procedure consisted of determining the system transport capability for an unprimed artery as a function of the liquid level below the evaporator. The artery was maintained in the unprimed condition by three methods. First, the connection between the artery and the jet pump was pinched shut. Secondly, the artery was plugged along its entire length which prevented liquid from filling the artery. The last method used was to physically disconnect the artery from the jet pump while leaving the artery intact in the evaporator tube. The first method was unreliable since it sometimes caused priming by thermal pumping (see Section 3.4). The second and last methods both created a truly unprimed artery.

The second step was then to determine transport capability with the primed artery and at the same time to observe the pumping of liquid. During all tests, the system was first set at some liquid level and then brought up at low power to the operating temperature ($66^{o}C$). Then the heater input was gradually increased until either burnout occurred or some other limit was reached. The jet pump was designed to provide a pumping pressure differential equal to the capillary head of 200-mesh screen (21 cm) at a throughput of 200 watts at the vapor temperature of $66^{o}C$.

At power levels of approximately 100 watts, a drop of the liquid level at the evaporator was always observed. The liquid drop resulted from venturi head losses which, in turn, caused the liquid level in the condenser to rise. Another reason for the drop in the evaporator level was in the filling of the artery. At power levels in excess of 200 watts and with the artery filled, venturi head losses were substantially increased because of liquid mass injection into the main flow.

The rise of the liquid in the condenser caused an operational problem. The liquid blocked part of the available condenser surface, and the heat rejection capability of the system was decreased. This blockage was one reason for changing to the second condenser design. In this design the condenser was located high enough so that it was never blocked with liquid. Another undesirable side effect of the condenser blockage was the subcooling of the liquid within the blocked portion of the condenser.

This was also eliminated by the new condenser design. However, subcooling was not entirely eliminated due to heat losses in the return lines.

With the artery connected to the jet pump, liquid was observed at the sight glass during almost all tests when the heater power exceeded 200 watts. Depending on the liquid level, the artery sight glass was located 13 to 18 cm above the pool. Based on the venturi test with air, a rise of the liquid of 18 cm corresponds to a power of 160 watts. Thus, a liquid rise up to the sight glass at 200 watts is not too far off predictions.

During some tests, liquid was observed to completely fill the sight glass. This always occurred at very high power levels. Liquid injection into the main vapor stream was then evident because of the substantial increase in the measured venturi head loss. During other tests, vaporization of the pumped liquid within the artery connections occurred. This resulted in alternating injections of liquid and vapor slugs. This mode of operation caused oscillations of the evaporator liquid level. The oscillations were attributed to the variation of venturi head loss depending on whether liquid or vapor was injected. During some tests, small gas or vapor bubbles were observed through the sight glass to travel with the pumped liquid.

In summary, the jet pump almost always pumped liquid or a combination of liquid and vapor up to the sight glass. The problems which plagued the test program were inconsistency and poor repeatability. Some of the problems were found to be caused by poor wetting (the wick had to be reoxidized a number of times) and by poor contact between the artery bridges and the outer wick. But the major source of problems was the fact that the test loop was not completely isothermal. Once the new condenser had been installed (which reduced the subcooling of the returning liquid from about $36^{o}C$ to $9^{o}C$) the test results became much more repeatable. But even then, some vaporization was still observed in the connecting tube between the artery and the venturi. Insulating all exposed lines also improved the behavior. It is believed that most or all problems were associated with this particular test loop and would not exist in an actual heat pipe.

## IV-3.2 Improved Transport Capability

A more quantitative demonstration of the jet pump's performance is in the increase in heat transport capability associated with a primed artery. Figure IV-4 shows the system performance as a function of liquid level for both the primed and unprimed artery. The experimental data was obtained with the artery physically disconnected or plugged. The predicted curve (Figure IV-4) shows the calculated performance with the artery deprimed. An actual burnout was never reached with the artery connected. In Figure IV-4, three performance points are shown for the primed artery. Each one is representative of a different liquid level at zero power. In each case, the level dropped with increasing power until it reached the bottom of the artery (at which point the artery must deprime). Thus, the maximum power which was carried was not indicative of a true transport limit but rather of a forced depriming of the artery due to depletion of liquid. The depression of the liquid level was mainly due to head loss in the jet pump at high powers and, additionally, due to trapping of liquid in the condenser. As can be expected, the ultimate power which the loop could carry was dependent on the initial liquid level. The higher the initial level, the higher the power at which complete depletion occurs. However, note that the levels at failure which are shown in Figure IV-4 are always at or close to the bottom of the artery.

In summary, the transport capability of the primed artery is at least 360 watts at a working liquid level of 6.5 to 7.0 cm below the heater. Figure IV-4 also shows the calculated performance with the artery unprimed for this particular wick configuration. The equations for this theoretical curve are presented in the Appendix. The theoretical model predicts lower performance than measured at every liquid level. The apparent discrepancy can be attributed to three factors: heat losses, condensation in the venturi, and contribution by liquid fillets. The system heat loss was not calibrated but is estimated to be in the range of 10 to 15 watts. Condensation above the evaporator and below the venturi would occur in a nonisothermal system. The condensate would gravity feed the top portion of the wick, allowing an increase in the apparent transport capability of the wick. The third and most significant factor is the presence of fillets. The placement of the artery inside the pipe lends itself to trapping

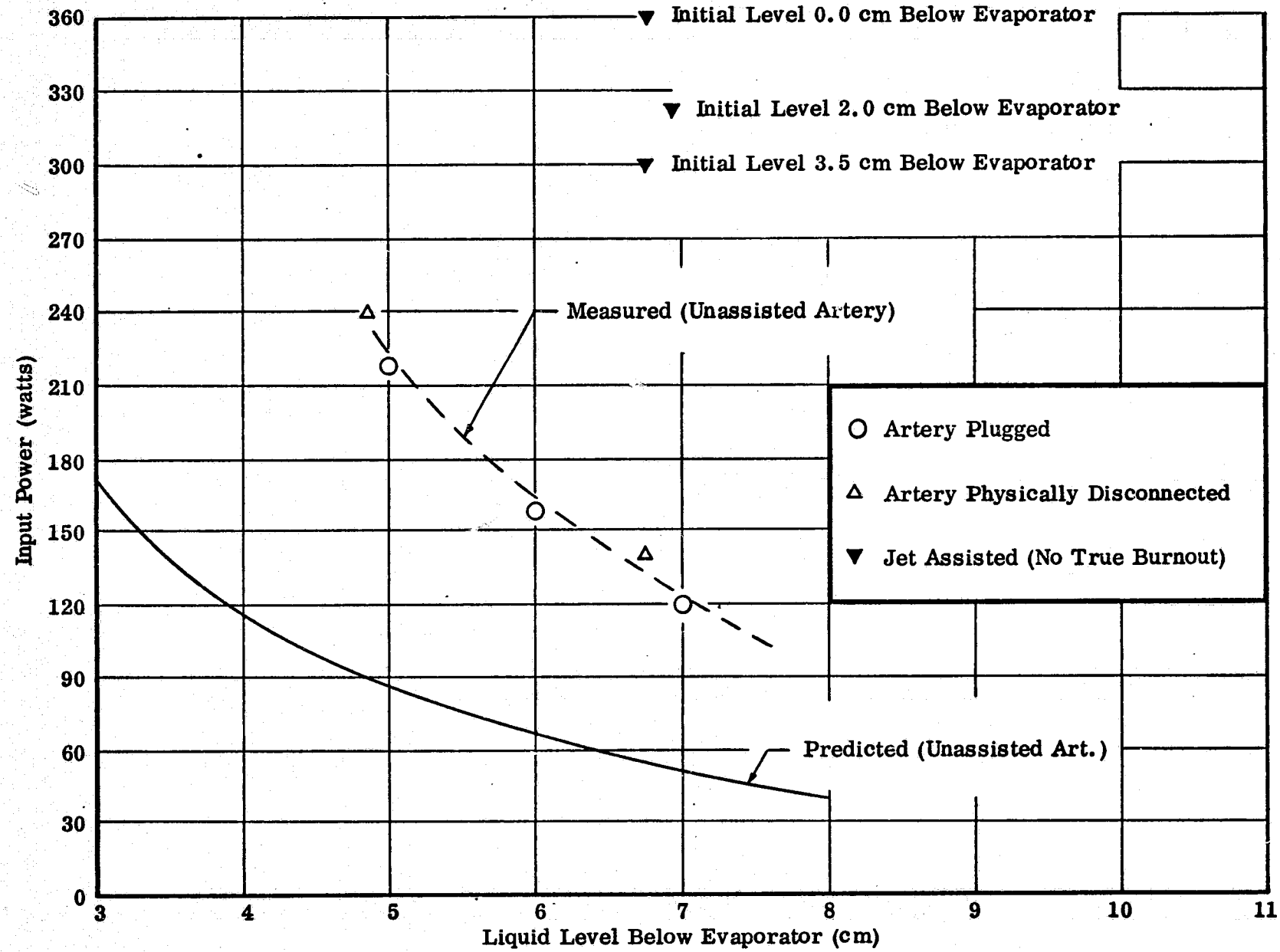


FIGURE IV-4

PERFORMANCE OF ARTERY WITH AND WITHOUT JET PUMP ASSISTANCE

fillets of liquid. The fillets themselves do not have significant pumping capability but they provide an additional source of liquid from which the evaporator can draw.

### IV-3.3 Recovery From Burnout

An interesting demonstration of the effectiveness of the jet pump was provided when a recovery from a partial burnout of the wick was achieved. During one test, with the jet pump connection pinched off, the system power input was slowly brought up to 200 watts at which power the wick began to burn out. At 220 watts, the top portion of the wick was burned out completely. Under this condition, the pinch was removed allowing the jet pump to prime the artery. The top portion of the wick immediately began to recover. The system was allowed to stabilize at 220 watts for one hour until complete recovery was accomplished. The power was then slowly increased to approximately 300 watts without any evidence of a burnout. Figure IV-5 shows the measured evaporator $\Delta T$ during the described various phases of this particular test. As a countercheck, the system was retested at the liquid level of the Figure IV-5 test but with the jet pump connected. The system input power was increased slowly up to 250 watts. At an input power of 250 watts, the jet pump connection was pinched off and burnout was immediately experienced in the evaporator.

### IV-3.4 Thermal Pumping

Thermal pumping is a phenomenon which exists as the result of temperature differences within an arterial heat pipe system. It is equivalent to "Clapeyron" priming which has been employed beneficially in the past. The artery, consisting of several layers of wet screen, is essentially isolated from the vapor in the evaporator section. If the artery is pinched it becomes a closed system; hence, the pressure inside the artery and, therefore, the liquid level is determined by the temperature of the liquid in the artery. If the temperature difference between the liquid inside the artery and the vapor outside the artery is not equalized by heat leaks (or mass flow through the jet), thermal pumping could cause the artery to prime even without the assist of the jet pump.

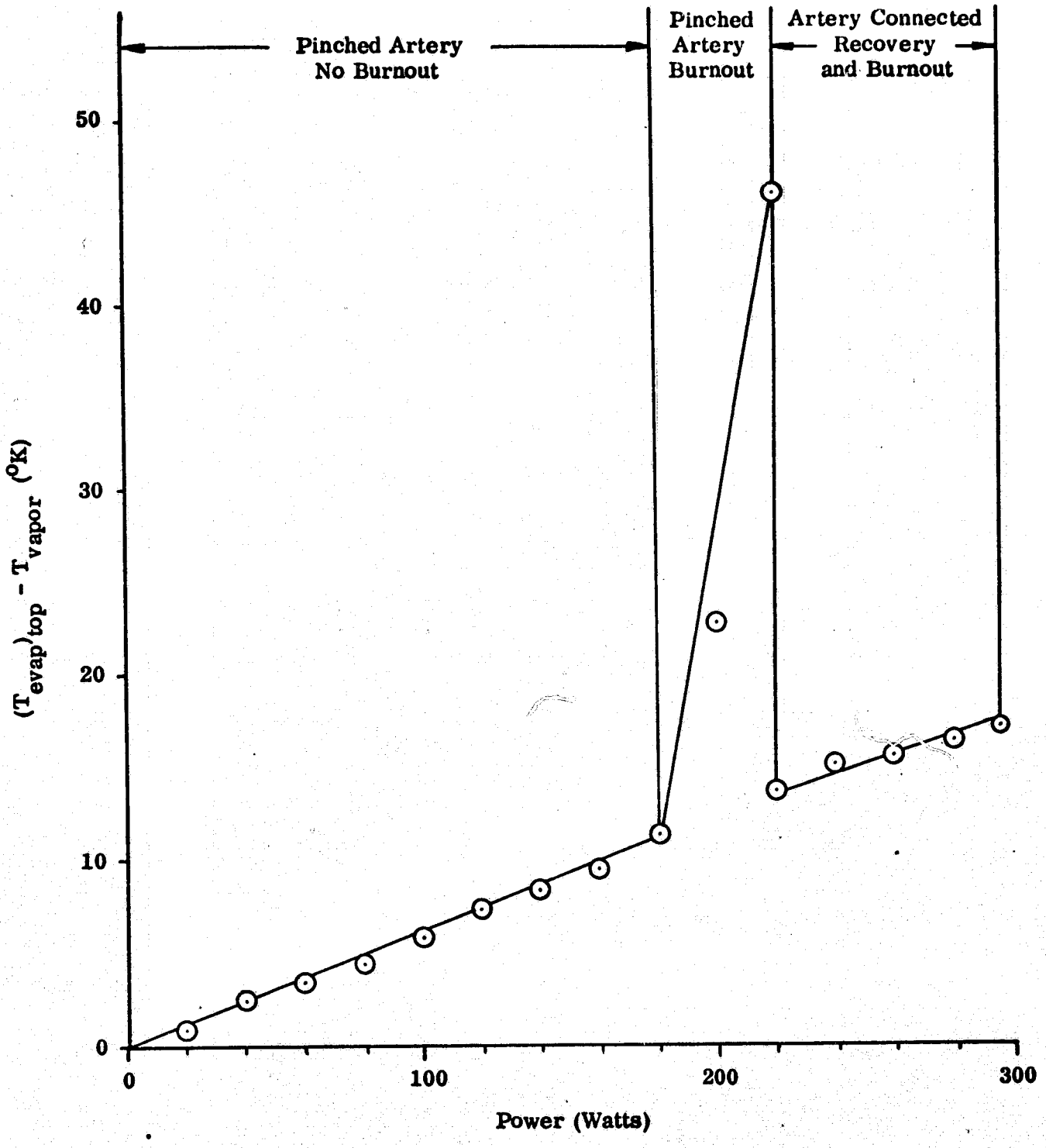


FIGURE IV-5

JET ASSISTED RECOVERY FROM BURNOUT

This phenomenon was evident during initial tests when the returning liquid was substantially subcooled. Modification of the condenser decreased the subcooling of the liquid but did not completely eliminate it. Thus, any tests with the artery pinched were always somewhat suspect of contributions due to thermal pumping. Therefore, the artery was either disconnected or plugged during all control tests when the performance without the aid of the jet pump was being evaluated. When the artery was connected to the jet pump, thermal pumping could not contribute to the performance. Under this condition, the vapor within the artery is in equilibrium with the state of the vapor at the throat of the venturi and any temperature and pressure imbalances are quickly equalized through mass flow. Thus, the observed performance with the jet pump is believed to be truly representative of an actual heat pipe system.

## V. CONCLUSIONS AND RECOMMENDATIONS

The objective of this program was to explore a new concept for priming arterial heat pipes. It utilizes a capillary driven jet pump to pump vapor and gas from the artery and fill it with liquid. The suction by the pump continues during normal heat pipe operation so that any noncondensible gas is continuously removed. In order to provide a proof-of-principle, a simple capillary loop was developed which was tested with water as the working fluid. It was instrumented for first order quantitative measurements and equipped with sight glasses for visual observations. The test results obtained from this experiment have verified the basic concept in a number of ways:

- Liquid was observed to fill the artery against a gravity head.
- A substantial increase in performance was obtained when the jet pump was operating.
- It was shown that the jet pump was capable of recovering a partially dried out wick.

The results of this exploratory effort suggest additional development work. The goal of this development will be a functional arterial heat pipe which is primed by a capillary jet pump. The following program tasks are recommended to reduce the concept to practice.

### Task I - Jet Pump Technology Development

The experimental proof-of-principle work has indicated several areas where additional basic development is needed before incorporating a jet pump into an actual heat pipe. First, a venturi, with a geometry which is typical for a jet pump assisted heat pipe, will be performance tested with a two phase flow system. During these tests, the effects of vapor and liquid addition on venturi performance need to be studied. Various venturi geometries must be investigated in order to optimize the jet pump. The experimental results will be correlated with the analytical model and the model adjusted as required.

The stability of the liquid and the vapor phases in the artery and the connections between artery and jet pump will be evaluated experimentally. Particularly, the effects of superheating and subcooling in the connections will be investigated.

Another objective of this task will be the development of the analytical model for the entire arterial heat pipe system including the priming requirements of typical arteries. As a result of this task, the necessary analytical tool for designing and optimizing a jet pump assisted heat pipe will be available.

Task II - Breadboard Jet Pump Assisted Heat Pipe

During this task a capillary jet pump will be incorporated into a working heat pipe. The heat pipe would be typically 2.5 cm in diameter and 1.0 m long. Ammonia is the best candidate working fluid but initial testing is best done with water. The heat pipe will be of modular design so that components can be readily exchanged or modified. Optimization of wick, artery, or jet pump will not be attempted at this stage. Instead, the objective will be a demonstration that reliable priming of an artery can be achieved by means of a jet pump. Tests will be conducted with pure working fluid and with a mixture of working fluid and noncondensible gas. The priming studies will be performed at various loads and orientations with respect to gravity.

Task III - Prototype Jet Pump Assisted Heat Pipe

The objective of this task is to incorporate a jet pump into an arterial heat pipe which is typical for aerospace applications. The artery design will be selected on the basis of adaptability to a jet pump and in accordance with NASA needs for future flight applications. At first, a detailed design study and analysis will be conducted. Options such as single versus multiple venturi will be considered. The heat pipe will then be fabricated and performance mapped. The test program will include steady-state and transient performance and operation with and without a condensible gas.

## VI. REFERENCES


1. Kroliczek, E., and Bienert, W., "Experimental High Performance Heat Pipes for the OAO-C Spacecrafts," ASME 71-Av-26

2. Enninger, James E., "Flight Data Analysis and Further Development of Variable-Conductance Heat Pipes," January 8, 1975, TRW 26263-6009-RU-00

3. Kosson, R., "A Tunnel Wick 100,000 Watt-Inch Heat Pipe," AIAA, 1972

## APPENDIX A

## DERIVATION OF PERFORMANCE EQUATION

The basic heat pipe performance equation is given in the Heat Pipe Design Handbook. It can be adapted easily to analytically describe the transport capability of the multiwick system shown schematically in Figure A-1. The liquid pressure gradient in the y direction is given by:

$$\frac{dP_l}{dy} = \frac{\mu_l \dot{m}(y)}{\rho_l K A} - \rho_l g \qquad \text{A-1}$$

Integrating this expression gives the total liquid pressure loss:

$$\Delta P_l = -\int_0^{h + L_{evap}} \left( \frac{\mu_l \dot{m}(y)}{\rho_l K A} + \rho_l g \right) dy \qquad \text{A-2}$$

The capillary head is given by:

$$\Delta P_{cap} = \frac{2\sigma}{r} \qquad \text{A-3}$$

Assuming no vapor losses, the force balance equation becomes:

$$\Delta P_{cap} + \Delta P_l = 0 \qquad \text{A-4}$$

or:

$$\frac{2\sigma}{r} = \int_0^{h = L_{evap}} \left( \frac{\mu_l \dot{m}(y)}{\rho_l K A} \right) dy + \rho_l g (h + L_e) \qquad \text{A-5}$$

The mass flow in the adiabatic section is given by:

$$\dot{m}(y) = \frac{Q_{max}}{\lambda} \qquad \text{A-6}$$

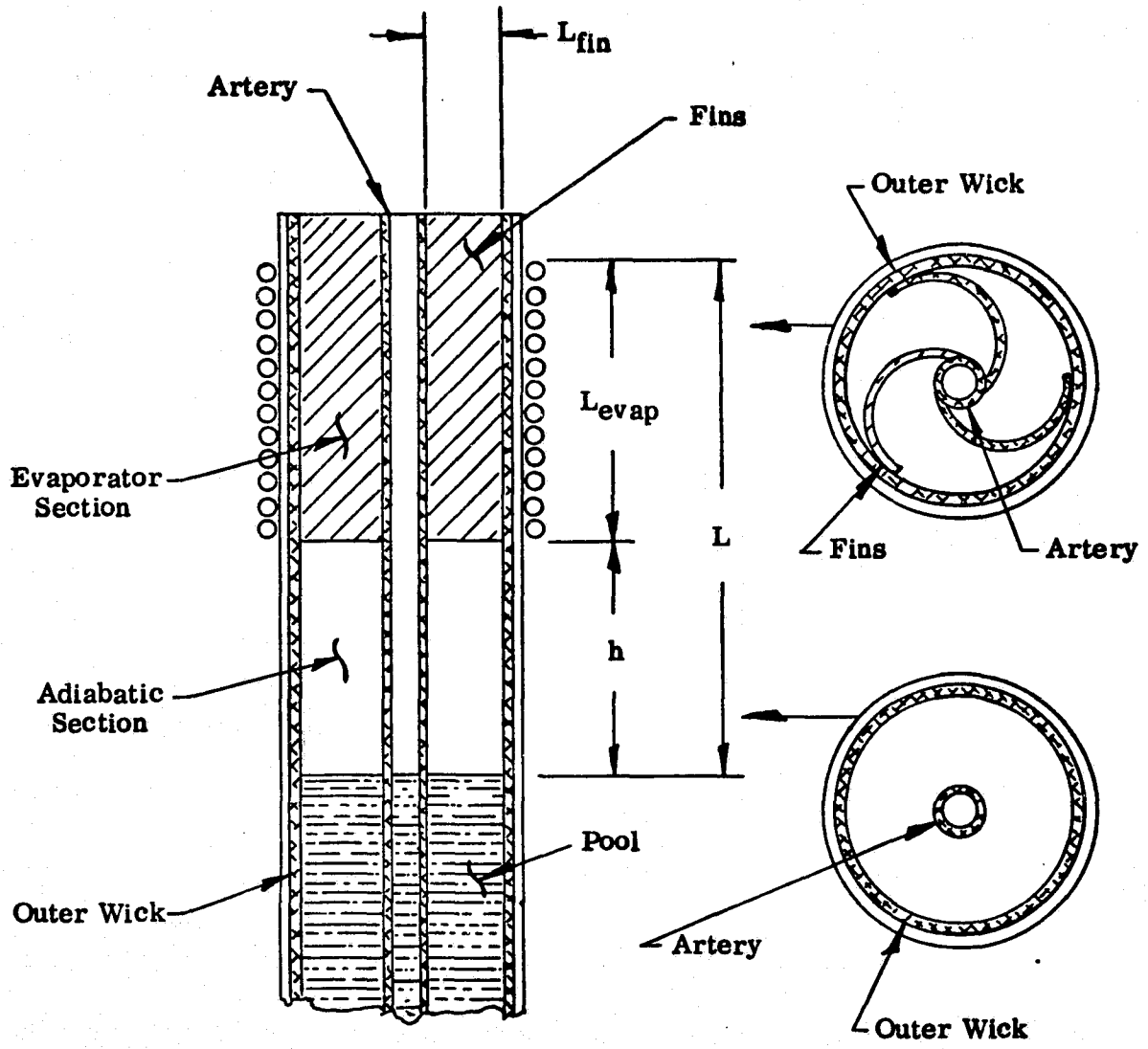


FIGURE A-1

GEOMETRY OF EVAPORATOR AND ADIABATIC SECTIONS

and in the evaporator section, it is given by:

$$\dot{m}(y) = \frac{Q_{max}}{\lambda}\left(\frac{(h + L_e)}{L_e} - \frac{y}{L_e}\right) \qquad \text{A-7}$$

Equation A-5 can be solved for Q, rearranged, and written as:

$$Q_{max} = \frac{2 N_l}{r} \frac{(1 - \eta)}{\left[\left(\frac{L}{KA}\right)_{adiabatic} + \left(\frac{L}{KA}\right)_{evap}\right]} \qquad \text{A-8}$$

where:

$$\eta = \frac{r (L_e + h)}{2 H} \qquad \text{A-9}$$

$$H = \frac{\sigma}{\rho_l g} \qquad \text{A-10}$$

$$N_l = \frac{\rho_l \lambda \sigma}{\mu_l} \qquad \text{A-11}$$

The evaporator area is given by:

$$A_{evap} = A_{fins} + A_{artery} + A_{outer\ wick\ evap} \qquad \text{A-12}$$

The adiabatic section area is given by:

$$A_{adiabatic} = A_{artery} + A_{outer\ wick\ adiabatic} \qquad \text{A-13}$$